Developmental Biology 445 (2019) 271–279

Contents lists available at ScienceDirect

Developmental Biology

journal homepage: www.elsevier.com/locate/developmentalbiology

Role of caveolin-1 in epidermal stem cells during burn wound healing in rats

Ronghua Yang[a,1], Jingru Wang[a,1], Ziheng Zhou[b], Shaohai Qi[b], Shubin Ruan[a], Zepeng Lin[a], Qi Xin[a], Yan Lin[a], Xiaodong Chen[a,*], Julin Xie[b,*]

[a] Department of Burn Surgery, the First People's Hospital of Foshan, Foshan 528000, Guangdong, China
[b] Department of Burn Surgery, First Affiliated Hospital of Sun Yat-Sen University, Guangzhou 510000, Guangdong, China

ARTICLE INFO

Keywords:
Epidermal stem cell
Caveolin-1
Burn
Skin wound healing
Epidermal growth factor
Mice

ABSTRACT

Local transplantation of stem cells has therapeutic effects on skin damage but cannot provide satisfactory wound healing. Studies on the mechanisms underlying the therapeutic effects of stem cells on skin wound healing will be needed. Hence, in the present study, we explored the role of Caveolin-1 in epidermal stem cells (EpiSCs) in the modulation of wound healing. We first isolated EpiSCs from mouse skin tissues and established stable EpiSCs with overexpression of Caveolin-1 using a lentiviral construct. We then evaluated the epidermal growth factor (EGF)-induced cell proliferation ability using cell counting Kit-8 (CCK-8) assay and assessed EpiSC pluripotency by examining Nanog mRNA levels in EpiSCs. Furthermore, we treated mice with skin burn injury using EpiSCs with overexpression of Caveolin-1. Histological examinations were conducted to evaluate re-epithelialization, wound scores, cell proliferation and capillary density in wounds. We found that overexpression of Caveolin-1 in EpiSCs promoted EGF-induced cell proliferation ability and increased wound closure in a mouse model of skin burn injury. Histological evaluation demonstrated that overexpression of Caveolin-1 in EpiSCs promoted re-epithelialization in wounds, enhanced cellularity, and increased vasculature, as well as increased wound scores. Taken together, our results suggested that Caveolin-1 expression in the EpiSCs play a critical role in the regulation of EpiSC proliferation ability and alteration of EpiSC proliferation ability may be an effective approach in promoting EpiSC-based therapy in skin wound healing.

1. Introduction

Stem cells have been reported for burn treatment in recent years. Recent studies have shown that systemic transplantation or local transplantation of stem cells has therapeutic effects on skin damage (Kanji and Das, 2017), can promote skin wound healing, endothelial cell transformation and vascular formation (Chen et al., 2009; Kanji and Das, 2017). However, studies also indicated that simple stem cell transplantation treatment cannot provide satisfactory wound healing. Hence, studies on the mechanisms underlying the therapeutic effects of stem cells on skin wound healing will be needed.

Our lab recently has shown that epidermal stem cells (EpiSCs) play a critical role in skin wound healing (Liu et al., 2016; Shi et al., 2015; Wang et al., 2017). Among many potential mechanisms of this process, Caveolin may deserve further investigation. Caveolin mainly have three subtypes, caveolin-1, caveolin-2, and caveolin-3, of which caveolin-1 is ubiquitous in various cell types (Williams and Lisanti, 2004). Caveolin-1 is an integral membrane protein on the cell membrane and is highly expressed in many cells. Previous studies have suggested that the function of caveolin-1 may be mainly involved in transmembrane transport, but recent studies have also shown that caveolin-1 can interact with a variety of proteins and is a signal transduction hub for cell signaling molecules (Boscher and Nabi, 2012; Fridolfsson et al., 2014). For example, various signaling molecules interact with the scaffold region of caveolin-1, such that the activity of the signaling protein molecule is inhibited to negatively regulate the signaling pathway. Additionally, caveolin-1 may also act as a regulatory molecule that may be involved in regulation of the activity of calcium channels. Given that stem cell proliferation and directed differentiation are regulated by various signal transduction and calcium signaling, suggesting that caveolin-1 may be involved in regulating the physiological activities of stem cells. For example, several studies in recent decades have found that caveolin-1 protein has been shown to promote the ability of cells to differentiate in specific directions in a variety of cells

* Corresponding authors.
E-mail addresses: chenxiaod111@sina.com (X. Chen), sysxiejl90@sohu.com (J. Xie).
[1] Those authors contributed equally to this work.

https://doi.org/10.1016/j.ydbio.2018.11.015
Received 25 September 2018; Received in revised form 22 November 2018; Accepted 22 November 2018
Available online 23 November 2018
0012-1606/

(Codenotti et al., 2016; Fu et al., 2012), and in particular, it has also been reported to regulate the differentiation fate of various stem cells including interstitial stem cells (Baker et al., 2012; Wang et al., 2013) and neural stem cells (Li et al., 2011a, 2011b).

Based on the above background, we postulated that caveolin-1 also regulates the physiological functions of EpiSCs, including proliferation and differentiation. Hence, we test the hypothesis that overexpression of caveolin-1 in EpiSCs promotes EpiSCs proliferation and differentiation and accelerates wound healing.

2. Materials and methods

2.1. Animals

Adult male and female BALB/c mice (~ 25 g) were obtained from Shanghai Laboratory Animal Center. All animals were maintained in a temperature- and humidity-controlled vivarium and were group-housed and were given ad libitum access to standard rodent diet at the Animal Research Center of First Affiliated Hospital of Sun Yat-Sen University under 12:12 h light/dark cycle. All animal experiments were approved by the Institutional Animal Care and Use Committee of First Affiliated Hospital of Sun Yat-Sen University. All experimental procedures, as well as behavioral and histological analyses were performed by experimenters who were blinded to the treatment conditions.

2.2. Mouse model of burn injury

The model of burn injury was established based on previous reports with minor modifications (Gurel et al., 2004; Zhu et al., 2008). We anesthetized mice using 1% pentobarbital (30 mg/kg) and shaved the hair on the back. A 10 × 10 mm of copper plate tip was attached to a 40 W soldering iron. The copper tip was connected to an electronic temperature controller to allow for precise temperature monitoring. The copper plat tip was heated to 100 °C and was vertically applied to the mouse skin for 10 s to induce the burn injury. Immediately following the burn injury, gauze was used to cover the wound. Gauze was pre-embedded in 22 °C isotonic saline, as described previously (Calum et al., 2014). After 5 min, each wound received intradermal injections of EpiSCs (blank LV-Cav-1 construct) or EpiSCs with overexpression of caveolin-1 (EpiSC-Cav-1). Four injections were conducted around the wound (0.8×10^6 in 20 μl of physiological saline solution per injection). In addition, the wound bed received 0.2×10^6 cells in 20 μl of growth factor-reduced Matrigel (BD Biosciences, Franklin Lakes, NJ, USA). Five minutes later, all mice were placed back to their individual home cage for recovery. Mice continued to have free access to rodent chow and tap water. Analgesia (30 mg codeine phosphate) was given during 24 h after burn injury in 500 ml tap water. We recorded wound healing using photographed images. Digital planimetry was used to measure wound area with ImageJ software (NIH, Bethesda, MD, USA). We then used the methods that have been reported previously to calculate wound closure rate and wound score (Shi et al., 2015)

2.3. Isolation of mouse EpiSCs

EpiSCs were isolated using established methods as described previously (Liu et al., 2016; Shi et al., 2015; Wang et al., 2017). Cells were allowed to adhere to the flasks and then collected and cultured in K-SFM medium in 5% CO_2 at 37 °C. Upon reaching 70–80% confluence, cells were then digested and passaged at a ratio of 1:2 (Reiisi et al., 2010). To characterize the cells, cells were evaluated with markers, including integrin-β1 (Cell Signaling Technology, Danvers, MA, USA) and CD34 (Santa Cruz Biotechnology, Dallas, TX, USA) by immunofluorescence staining (Eckert et al., 2013).

2.4. Immunofluorescence

A 6-well plate was used for cell culture. A number of 10^4 cells were placed in each well for 24 h. The cells were then rinsed with PBS for five times, followed by 15-min fixation using 4% paraformaldehyde solution at room temperature, and 5-min permeation using 0.5% Triton X-100-PBS solution. Cells were then blocked for 30 min using 3% BSA in PBS. Primary antibodies to CD 34 (rabbit polyclonal antibody, 1:50, Santa Cruz Biotechnology, Dallas, TX, USA) and β1 integrin (rabbit polyclonal antibody, 1:50, Cell Signaling Technology, Danvers, MA, USA) were then incubated with the cells were respectively overnight at 4 °C. The binding of primary antibody was detected using corresponding goat anti-mouse IgG FITC and goat anti-rabbit IgG: Cy3 (Cell Signaling Technology, Danvers, MA, USA). A fluorescence microscope was used to evaluate the staining.

2.5. Construction of pcDNA-CAV-1 for lentiviral expression

Total-RNA was extracted from mouse leukocytes, and we used PCR to amplify the cav-1 cDNA, which at both ends contains *Xba*I and *Bam*HI restriction sites. The fragment was digested and then inserted into pcDNA-EF1-GFP between the *Xba*I and *Bam*HI restriction sites to generate the recombinant pcDNA-CAV-1 plasmid. We then screened and sequenced the positive clone of the recombinant pcDNA-CAV-1 plasmid, followed by purification.

2.6. Viral production

The viral production was based on Tronolab protocols. Briefly, we used transient transfection of HEK293T cells to produce recombinant lentivirus. Transfer vector (20 μg), packaging plasmid (psPAX2; 15 μg) and envelope plasmid (pMD2.G; 6 μg) were used to co-transfected to sub-confluent HEK293T cells. After two days, supernatant received ultra-centrifuge (Beckman L-70; 29,850 ×*g*) for 2 h at 4 °C. The pellets were then resuspended in PBS (100 μl), and aliquoted to 20 μl fresh suspension for each experiment.

2.7. Establishment of EpiSCs with stable expression of Caveolin-1

Cav-1 lentiviral constructs were used to transduce mice EpiSCs using previously described methods (Robert-Moreno et al., 2008). Lipofectamine 2000 was the transfection reagent. Lentiviral vector overexpressing Cav1 with GFP signals were used to infect EpiSCs, we confirmed that over 80% of transfected cells were selected for further experiments.

2.8. Transfection of siRNA

The oligonucleotide pairs of Cav-1 small-interfering RNAs are complementary to exon 3 (GenBank accession no. NM_007616), and the sequences of the sense strands are 5′-CCAUCAAUUUG GAGACUAUtt-3′, 5′-CCACUCAGCAACUGAAUGAtt-3′ and 5′-GU ACCUGAGUCUCCAGAAAtt-3′, respectively. To negative control siRNA is 5′-ACGACTAGCCTGAACTCAA-3′. Upon reaching 70–80% confluency, EpiSCs cells were transfected with control siRNAs or specific Cav-1-siRNAs mixed with lipofectamine TM2000 (Invitrogen) according to manufacturer's recommendation. After 6 h at 37 °C, the medium was changed, and the cells were cultivated in K-SFM medium in 5% CO_2 at 37 °C.

2.9. Cell counting Kit-8 assay

To examine the proliferation of EpiSCs, EpiSCs were placed in 96-well plates at a density of 2×10^4 cells per well. EpiSCs were treated with collagen type IV, followed with epidermal growth factor (EGF; 0 or 10 ng/ml). We then added 10 μl of CCK-8 (Sigma-Aldrich, St. Louis,

MO) solutions to each well at post-seeding day 2, 4, 6, 8 and 10. Samples were then incubated for 2 h. A micro-plate reader (Thermo Fisher, Waltham, MA USA) was used to determine the specific absorbance at 450 nm (A_{450}). All of the experiments were independently repeated at least three times, and measurements from 5 duplicate wells were used to generate the average.

2.10. Western blot

At post seeding day 10, proteins were extracted from cell pellets and dissolved in RIPA cell lysis buffer containing a protease inhibitor cocktail and a phosphatase inhibitor cocktail (Sigma-Aldrich, St. Louis, MO). Protein concentrations were determined with a Bradford protein assay kit (Bio-Rad) and separated through 12% SDS-PAGE gels, followed by electrophoretic transfer to polyvinylidene difluoride (PVDF) membrane. The membranes were blocked in 5% BSA for 2 h, rinsed, and incubated overnight at 4 °C with primary anti-Cav-1 (Rabbit, 1:1000, Cell signal) in 5% BSA. Excess antibodies were removed by washing the membrane with TBS/0.1% Tween-20 and the membranes were incubated for 1 h with horseradish peroxidase-conjugated secondary antibodies. To normalize the amounts of proteins applied to SDS-PAGE, the membranes initially incubated with primary and secondary antibodies, were re-probed with β-actin (Mouse, 1:2000, Sigma) antibodies as internal references, respectively. The bands were visualized by advanced chemoluminescence (GE, Healthcare Life Sciences), recorded by Gel-Doc (Bio-Rad) and the relative band intensity was quantified by Quantity One software (Bio-Rad).

2.11. Endothelial cell network formation assay

We used human umbilical vein endothelial cells (HUVECs) for this assay. Cells were placed in each well at a density of 2.5×10^4 cells per well. Cells were suspended in epithelial cell growth medium-2 (0.4 ml) supplemented with the EpiSC-conditioned medium. Cells were then seeded onto 24-well plates coated with Matrigel (BD Biosciences, Franklin Lakes, NJ, USA), followed by 12-h incubation in 5% CO_2 at 37 °C. After disposing of the medium, the cells were fixed, and we took the images. The NIH Image J software was used to determine the total length of the tube-like structures. For each well, we made four random fields for measurements.

2.12. Quantitative real-time PCR

Total RNA was extracted from the wound tissue samples using Trizol Reagent (Invitrogen, Waltham, MA USA). We then used the PrimeScript RT reagent Kit (Takara, Dalian, China) to transcribe RNA into cDNA. Quantitative real-time PCR (qRT-PCR) was conducted in the QuantStudio 3 Real-Time PCR Systems (Thermo Fisher Scientific, Waltham, MA USA) using SYBR Premix ExTaq (Takara, Dalian, China) and the primer sequences for Nanog were as follows: forward, CCGTTGGGCTGACATGAGCGT and reverse, GGCAGGCATCGGC GAGGAAT; GAPDH (ab9485; Abcam, Cambridge, MA, USA) was used as internal control. The $2^{-\Delta\Delta CT}$ method was then used to calculate the relative expression ratio of mRNA. All the experiments were repeated 3 times.

2.13. Histological analysis and immunohistochemistry staining

In separate groups of mice, skin tissue samples were collected at post-injury day 7, and fixed with formalin, embedded in paraffin, and sectioned at 4 μm thickness. Standard light microscopy (OLYMPUS, Tokyo, Japan) was used to evaluate H & E staining. Wound score ranging from 1 to 10 was given to each slide. For immunofluorescence, endothelial cells were stained with anti-CD31 (ab28364, Abcam, Cambridge, MA, USA) followed by incubation with a biotinylated secondary antibody (Abcam, Cambridge, MA, USA). The stain was visualized with Fluor 568-conjugated streptavidin (Invitrogen, Waltham, MA USA). We also used the previously described methods to perform nuclear staining with Hoechst and Ki67 (Borue et al., 2004). A Zeiss LSM 510 confocal microscope (Carl Zeiss, Oberkochen, Germany) was used to examine the sections. The number of Ki67-positive nuclei and total nuclei in five random fields were used to calculate the percentages of Ki67-positive nuclei. Cell counting was conducted using NIH Image J. We also examined capillary density using immunofluorescence staining for endothelial cells marker CD31. The growth of new blood vessels in terms of their length, size and junction was calculated using AngioQuant software (image analysis tool for angiogenesis). All histological analysis was conducted by experimenters who were blinded to the experiment conditions.

2.14. Statistical analysis

We analyzed all data using PRISM5.0 software (GraphPad, CA, USA). Values were expressed as the mean ± standard deviation (SD). Because there was no difference in all data analysis between male and female groups, we combined male and female group data together. Student's *t*-test was used to compare the difference between control and experimental groups. One-way analysis of variance (ANOVA) or multi-factorial ANOVA was used for comparing the differences between multiple groups. A Bonferroni *post-hoc* test for pairwise comparisons was performed as appropriate. $P < 0.05$ indicates that the difference was statistically significant.

3. Results

3.1. Effects of overexpression or knockdown of Caveolin-1 on the proliferative ability of EpiSCs

The cells that we isolated demonstrated typical morphology of EpiSCs (Fig. 1A). We used immunofluorescence to examine the expression of CD34 (Fig. 1B) and β1 integrin (Fig. 1C). The proliferative ability of EpiSCs infected with Lv-Cav-1 was similar to the control without EGF treatment. However, after we treated EpiSCs with EGF, and observed that it increased the proliferation of EpiSCs compared to vehicle control (treatment main effect, $p < 0.01$; Fig. 1D). Furthermore, we found that overexpression of Caveolin-1 in EpiSCs promoted the proliferation of EpiSCs compared to control EpiSCs (blank lentiviral construct) (EpiSC and treatment interaction effect, $p < 0.05$, Fig. 1D). We also examined the role endogenous levels of Caveolin-1 in regulation of the proliferative ability of EpiSCs. The proliferative ability of EpiSCs infected with Caveolin-1 siRNAs was similar to the control without EGF treatment. However, after we treated EpiSCs with EGF, we found that it slightly increased the proliferation of EpiSCs compared to scramble siRNA control (treatment main effect, $p < 0.01$; Fig. 1E). Furthermore, we found that knockdown of Caveolin-1 in EpiSCs decreased the proliferation of EpiSCs compared to control EpiSCs (scramble siRNA) (EpiSC and treatment interaction effect, $p < 0.05$, Fig. 1E). We also verified the protein levels of Caveolin-1 in each treatment group and found that Lv-Cav-1 treatment enhanced Caveolin-1 expression (Fig. 1F), and Cav-1 siRNAs treatment decreased Caveolin-1 expression (Fig. 1G). In addition, EGF treatment (10 ng/ml) did not alter Caveolin-1 expression as compared to control (o ng/ml). To assess the effects of over-expression of Caveolin-1 on EpiSC pluripotency, we used RT-PCR to assess the change in expression of Nanog during the EpiSC differentiation process induced by EGF. We found that Nanog mRNA expression decreased overtime (Fig. 1H). However, overexpression or knockdown of Caveolin-1 in EpiSCs did not alter Nanog expression compared to control EpiSCs (Fig. 1H).

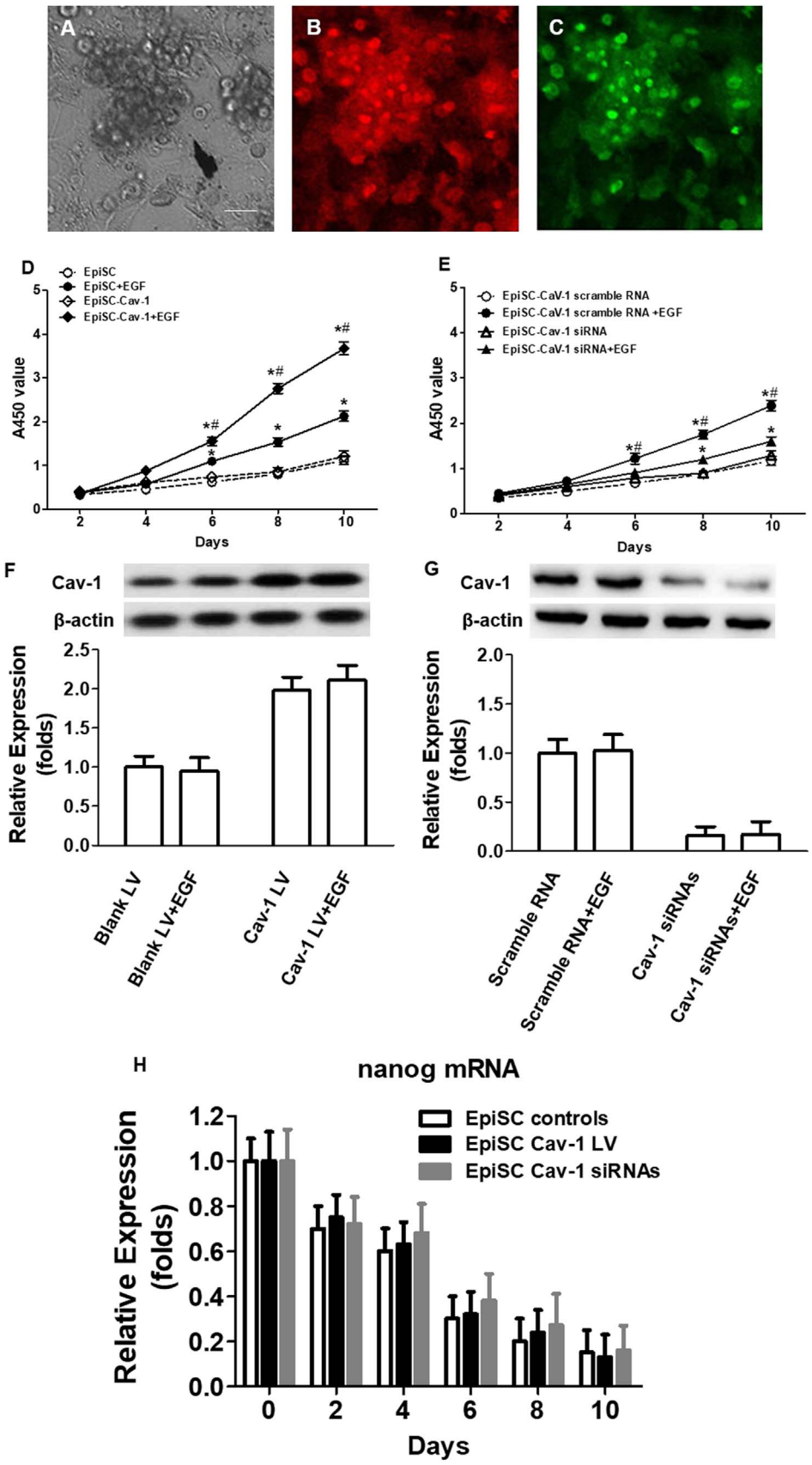

Fig. 1. Effects of overexpression or knockdown of Caveolin-1 on EpiSC proliferation and differentiation. (A) The morphology of the isolated cells. **(B)** The isolated cells positively express CD34 and **(C)** β1 integrin as detected by immunofluorescence. **(D)** EpiSCs that have Caveolin-1 overexpression were treated with EFG (0 or 10 ng/ml) for 10 days and showed increased proliferation. **(E)** EpiSCs that were treated with Caveolin-1 siRNAs were treated with EFG (0 or 10 ng/ml) for 10 days and showed increased proliferation. **(F)** EpiSCs were treated with lentivirus and EFG (0 or 10 ng/ml) for 10 days and the protein levels of Caveolin-1. **(G)** EpiSCs were treated with Caveolin-1 siRNAs and EFG (0 or 10 ng/ml) for 10 days and the protein levels of Caveolin-1. (**H**) mRNA expression of nanog. Scale bar = 20 μm. Asterisks represent single treatment effect compared to vehicle (i.e., 0 ng/ml EFG), $p < 0.05$. Ponds represent significant effect compared to non-Cav-1 overexpression EpiSCs, $p < 0.05$.

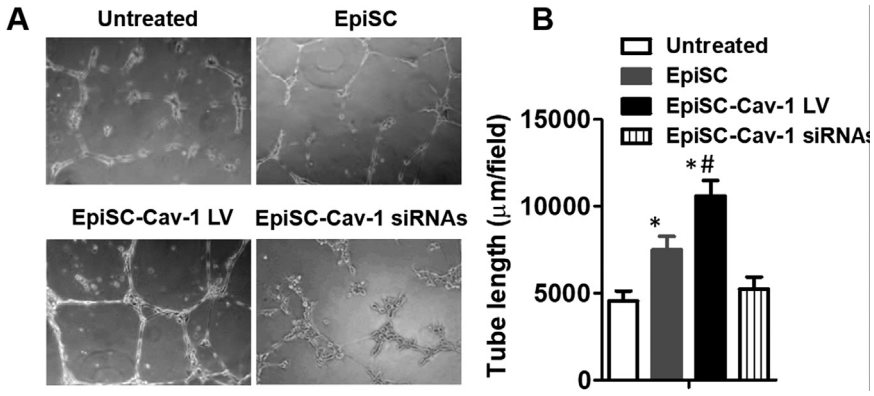

Fig. 2. Effects of EpiSC-conditioned medium on human umbilical vein endothelial cells (HUVECs). Endothelial cell tube formation. HUVECs were suspended in vehicle-, EpiSC-, EpiSC-Cav-1-LV, or EpiSC-Cav- siRNAs conditioned EGM-2 medium, which contained growth factor cocktail and 2% FBS, and incubated for 24 h. (A) Representative fields are shown. (B) The total length of the tube network per field was quantified. Experiments were performed in triplicate wells. Asterisks represent significant difference compared to vehicle (i.e., untreated), $p < 0.05$. Ponds represent significant difference compared to EpiSCs, $p < 0.05$.

3.2. Effects of overexpression or knockdown of Caveolin-1 in EpiSC on endothelial cell tube formation

We found that incubation of human umbilical vein endothelial cells (HUVEC) with EpiSC-conditioned medium enhanced tube formation of HUVEC on Matrigel compared with vehicle control medium (i.e., untreated; Fig. 2). Furthermore, after overexpression of Caveolin-1 in EpiSCs using LV-Cav-1, incubation of HUVEC with EpiSC-conditioned medium promoted tube formation of HUVEC on Matrigel compared to EpiSC control medium (Fig. 2). Additionally, after knockdown of Caveolin-1 in EpiSCs using siRNAs, incubation of HUVEC with EpiSC-conditioned medium did not alter tube formation of HUVEC on Matrigel compared to EpiSC control medium (i.e., untreated; Fig. 2).

3.3. Effects of overexpression of Caveolin-1 in EpiSC on wound healing

We found that EpiSC-treated wounds exhibited accelerated wound closure in rats (treatment and day interaction effect, p < 0.05; Fig. 3A and B) compared with vehicle medium treated wounds. Furthermore, the wound closure rate was further increased in mice that received EpiSC-Cav-1 treatment (treatment and day interaction effect, Bonferroni post-hoc, p < 0.05; Fig. 3A and B).

Histological evaluation was then performed in separate groups of mice (n = 5/group) at post-injury day 7, when robust skin closure was observed. We found enhanced re-epithelialization in EpiSC-treated wounds compared with control medium-treated wounds (i.e., untreated; Fig. 4A). Furthermore, overexpression of Caveolin-1 in EpiSCs promoted re-epithelialization in wounds (Fig. 4A). Further analysis of wounds showed that EpiSC-treated wounds exhibited increased cellularity and vasculature (Fig. 4A and D). In addition, in EpiSC-treated wounds, granulation tissue was thicker and larger (Fig. 4A). Notably, EpiSC-Cav-1-treated wounds further demonstrated increased cellularity and vasculature, as well as thicker and larger granulation tissue (Fig. 4A and D). Consistent with these findings, the wound scores at post-injury day 7 were significantly higher in EpiSC-treated wounds (Fig. 4C). In addition, EpiSC-Cav-1-treated wounds appeared to have increased wound scores (Fig. 4C), suggesting enhanced wound healing. We then also measured cell division in the wound sections. As shown in Fig. 4B and E, EpiSC-treated wounds showed an increased percentage of Ki67-positive cells compared with control medium-treated wounds. Furthermore, EpiSC-Cav-1-treated wounds showed a further increase in the numbers of Ki67-positive cells (Fig. 4B and E).

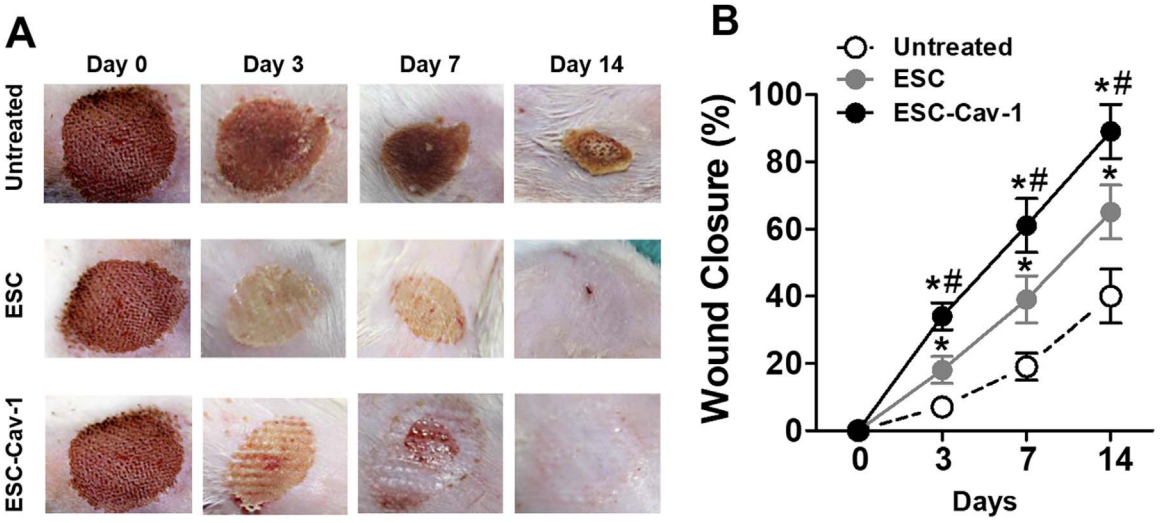

Fig. 3. Effects of EpiSC treatment on wound closure (n = 10/group). (A) Images of wounds in BALB/c mice over 14 days after burn injury. (B) Wound measurement of in three treatment groups. Asterisks represent single treatment effect compared to vehicle (i.e., 0 ng/ml EFG), $p < 0.05$. Ponds represent single Cav-1 expression effect compared to non-Cav-1 overexpression EpiSCs, $p < 0.05$.

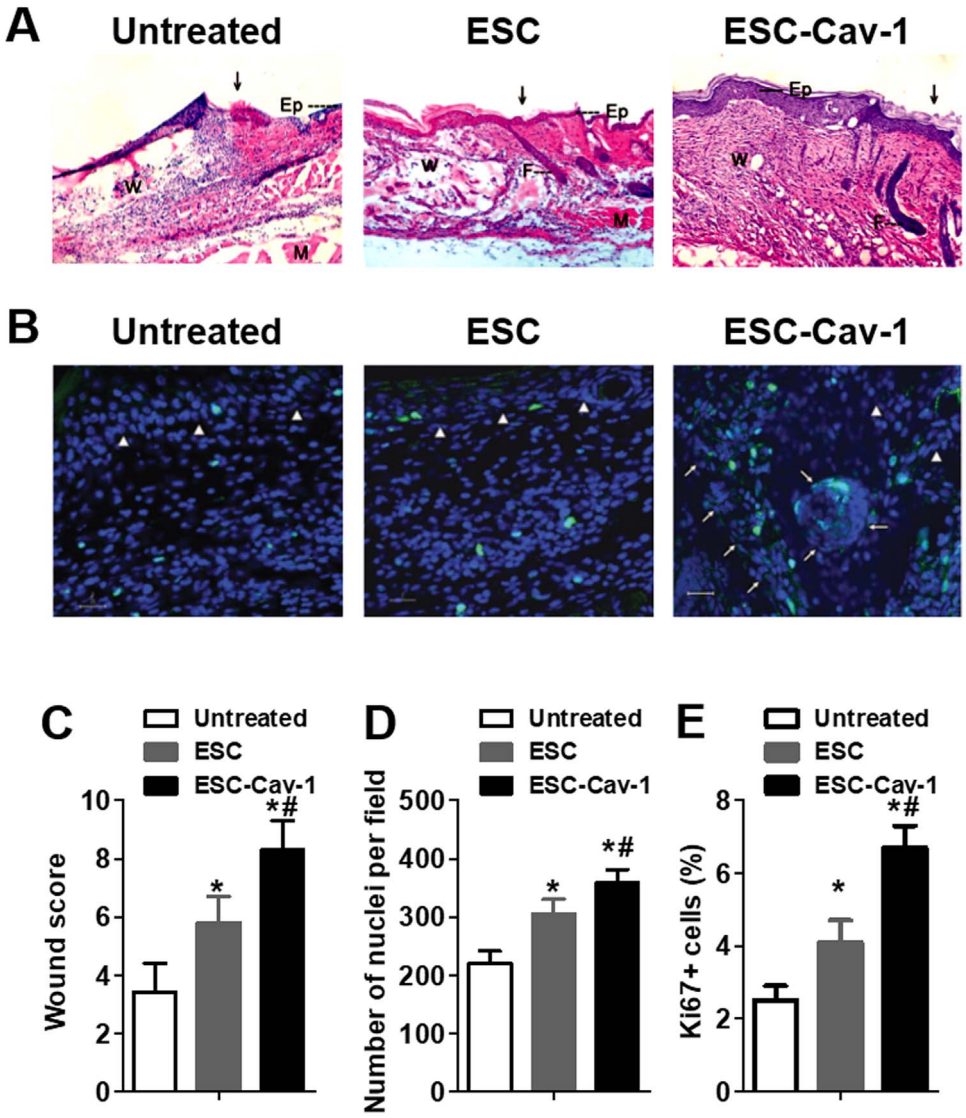

Fig. 4. Histological analysis of wound healing in BALB/c mice at post-injury day 7 (n = 5/group). (A) Wound histological images (H & E stain). Arrows indicate wound edges. (B): Confocal images of Ki67 (green) and Hoechst (blue) stain of wounds at post-injury day 7. Arrowheads indicate the epidermis or wound surfaces. Arrows indicate Ki67-positive skin appendages. Scale bar = 20 μm. (C): Wound histological scores at post-injury day 7. (D) Wound cellularity was determined by counting the number of nuclei per high-power (×400) field. (E) Percentages of Ki67-positive cells in wounds at post-injury day 7. Ep = epidermis; F = hair follicle; M = muscle; W = wound bed. Asterisks represent single treatment effect compared to vehicle (i.e., 0 ng/ml EFG), $p < 0.05$. Ponds represent single Cav-1 expression effect compared to non-Cav-1 overexpression EpiSCs, $p < 0.05$.

3.4. Effects of overexpression of Caveolin-1 in EpiSC on angiogenesis

Our in vitro studies on HUVEC indicated that EpiSC treatment may enhance angiogenesis. Hence, conducted macroscopic visualization of blood vessels. We found that blood vessel surrounded the wounds in the skin in EpiSC-treated wounds at post-injury day 7 in mice compared to vehicle control medium-treated wounds (Fig. 5A). Furthermore, more vessels and vessel branches were found in wounds in EpiSC-Cav-1-treated wounds at post-injury day 7 in BALB/c mice (Fig. 5A).

To confirm these findings, we performed immunohistological staining for endothelial protein CD31 and assessed capillary densities in wounds at post-injury day 7. We found that CD31 staining was increased in wounds treated with EpiSCs (Fig. 5B). In addition, EpiSC-Cav-1-treated wounds showed further increased CD31 staining compared to EpiSC-treated wounds (Fig. 5B). Finally, capillary density was calculated and was consistent with the results of CD31 staining. Specifically, we found that capillary density was increased in wounds treated with EpiSCs (Fig. 5C). In addition, EpiSC-Cav-1-treated wounds showed further increased capillary density compared to EpiSC-treated wounds (Fig. 5C).

Finally, the growth of new blood vessels in terms of their length, size and junction was calculated using AngioQuant software. We found that overexpression of Caveolin-1 in EpiSCs enhanced the blood vessel length (Fig. 5D), the size of vessels (Fig. 5E), and the number of junctions (Fig. 5F).

4. Discussion

In this study, we found that overexpression of Caveolin-1 in EpiSCs promoted EGF-induced cell proliferation ability, and knockdown of Caveolin-1 in EpiSCs reduced EGF-induced cell proliferation ability. This effect was associated with no alteration of Nanog mRNA in EpiSCs, suggesting Caveolin-1 overexpression did not alter EpiSC pluripotency. Furthermore, we found that incubation of HUVEC with EpiSC-Cav-1-conditioned medium promoted HUVEC tube formation, indicating a paracrine effect of EpiSC on angiogenesis. Based on these in vitro experimental results, we treated mice with skin burn injury using EpiSCs with overexpression of Caveolin-1. We found that wound closure rate was increased in mice that received EpiSC-Cav-1 treatment. Histological evaluation demonstrated that overexpression of

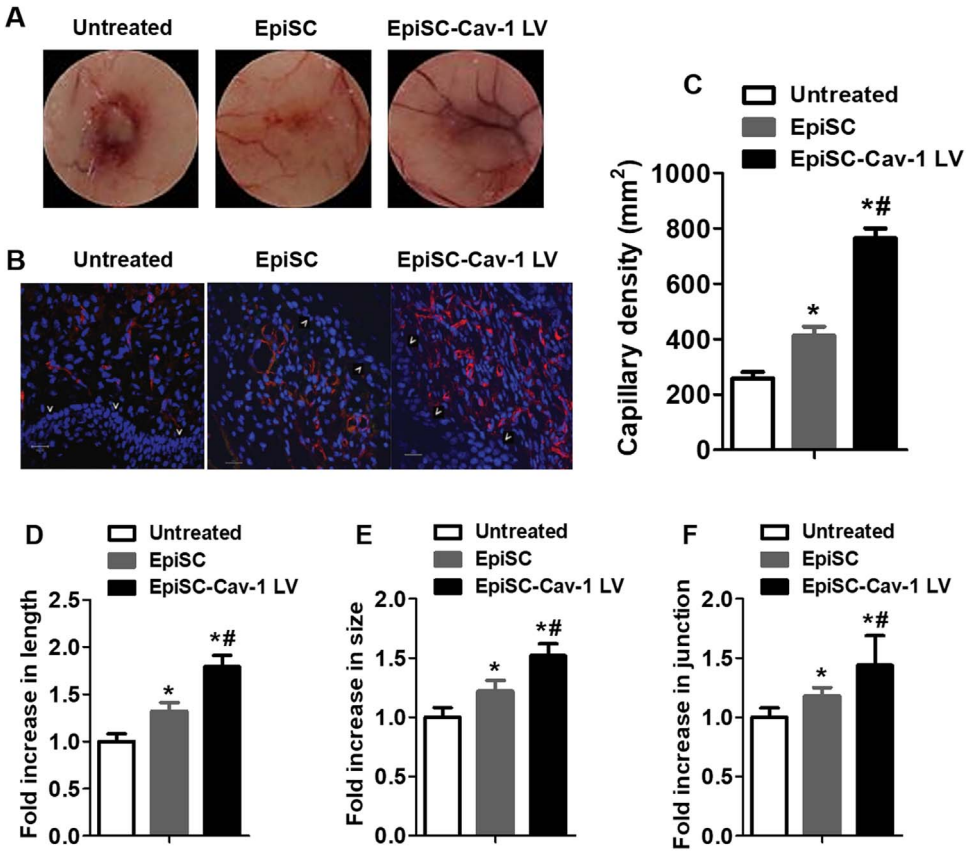

Fig. 5. Effects of EpiSC treatment on wound vascularity. (A) Representative images of skin wounds at post-injury day 7 in BALB/c mice. (B) Immunofluorescence for endothelial cells. Wound sections were stained with anti-CD31 antibody and detected with Fluor 568 (red). Nuclei were stained with Hoechst (blue). Arrowheads indicate the epidermis. Scale bar = 20 μm. (C) Capillary density was counted after CD31 staining. The growth of new blood vessels in terms of (D) their length, (E) size and (F) junction was calculated using AngioQuant software (image analysis tool for angiogenesis). Asterisks represent single treatment effect compared to vehicle (i.e., 0 ng/ml EFG), $p < 0.05$. Ponds represent single Cav-1 expression effect compared to non-Cav-1 overexpression EpiSCs, $p < 0.05$.

Caveolin-1 in EpiSCs promoted re-epithelialization in wounds, enhanced cellularity, and increased vasculature, as well as increased wound scores, suggesting enhanced wound healing. These effects were associated with increased proportions of Ki67-positive cells, suggesting enhanced in vivo cell proliferation in wounds. Finally, microscopic visualization and immunohistological staining for endothelial protein CD31 showed that overexpression of Caveolin-1 in EpiSCs increased capillary density in wounds treated with EpiSC-Cav-1. Analysis for angiogenesis found that overexpression of Caveolin-1 in EpiSCs increase the length, size, and junctions of blood vessels. Taken together, our results suggested that Caveolin-1 expression in the EpiSCs play a critical role in the regulation of EpiSC proliferation ability and factors secreted by EpiSCs can promote angiogenesis. Hence, alteration of ESC proliferation ability may be an effective approach in promoting ESC-based therapy in skin wound healing.

Re-epithelialization is necessary for restoring the epidermis during the repair of burn wounds. Our data showed that EpiCSs play a critical role in promoting re-epithelialization during this process. EpiSCs have high proliferation and differentiation potential and are found in the follicle bugle of hair and the basal layer of the epidermis (Charruyer and Ghadially, 2011). Under physiological conditions, EpiSCs are involved in maintaining the normal structure and function of the skin and play a critical role in wound repairing via proliferation, differentiation, and migration (Blanpain and Fuchs, 2009). Adding to this line of research, our results indicated that the expression of Caveolin-1 in EpiSCs is involved in the regulation of the process of re-epithelialization after skin wound injury. Notably, previous studies have shown that loss of caveolin-1 is associated with abnormal re-epithelialization in lung fibrosis (Odajima et al., 2007). Hence, future studies are necessary to investigate the specific mechanisms underlying this phenomenon.

Caveolin-1 is also involved in differentiated cell proliferation (Fujita et al., 2004; Galbiati et al., 2001). Studies have shown that increased numbers of cells expressing stem cell markers were found in many organs including gut, mammary gland and brain in caveolin-1 null mouse (Jasmin et al., 2009; Li et al., 2005; Sotgia et al., 2005), suggesting that caveolin-1 may play a negative role in the regulation of stem cell proliferation. Furthermore, Caveolin-1 can facilitate glucocorticoid receptor signaling leading to inhibition of proliferation in mouse neural progenitor cells (Samarasinghe et al., 2011). In addition, bone marrow-derived mesenchymal stem cells (MSCs) exhibited higher proliferative rate in culture after isolation from the Caveolin-1 null mouse (Case et al., 2010). Similarly, it has been shown that the proliferative rate of human MSCs is inversely associated with caveolin-1 expression (Park et al., 2005). Finally, knockdown of Caveolin-1 expression using siRNA in human MSCs increases their proliferation (Baker et al., 2012). However, in contrast to these findings, our results suggested that Caveolin-1 expression level in the EpiSCs is positively correlated with proliferation ability. Similar to our findings, it has been reported that treatment of mouse embryonic stem cells with Caveolin-1 siRNA reduces the cell proliferation index (Lee et al., 2010), and caveolae integrity and Caveolin-1 phosphorylation are necessary for downstream activation of DNA synthesis in embryonic stem cells (Park and Han, 2009; Park et al., 2011). Taken together, our findings with others suggested that the role of Caveolin-1 in the regulation of stem cell proliferation may involve complicated signaling pathways in difference stem cells.

Many studies have shown that cell differentiation is usually associated with increased Caveolin expression in vitro (Fuchs et al.,

2003; Ng et al., 2004), suggesting that Caveolin expression may inhibit cell differentiation. For example, in Caveolin-1 null mouse, bone marrow MSCs exhibited greater osteogenic potential (Rubin et al., 2007). In addition, caveolin-1 knockdown enhances human MSC osteogenesis (Baker et al., 2012) and adipogenesis (Park et al., 2005), as well as murine and rat neuronal differentiation (Li et al., 2011a, 2011c; Wang et al., 2013). Surprisingly, our results suggested that overexpression of Caveolin-1 in EpiSCs may not alter the differentiation potential of EpiSCs after treatment of EGF by assessing mRNA levels of Nanog. While we did not examine other stem cell differentiation markers, it is possible that different signaling pathways may be involved in different types of stem cells. For instance, rat MSC differentiation is regulated by caveolae endocytosis of BMP receptors (Du et al., 2011) and Caveolin-1 null mouse exhibited active β-catenin levels in cells expressing stem cell markers in both intestinal crypts and mammary gland (Li et al., 2005; Sotgia et al., 2005). In contrast, Caveolin-1 regulation of neurogenesis may occur via effects on Notch signaling (Wang et al., 2013). Our lab also demonstrated that EpiSCs can accelerate diabetic wound healing via the Notch signaling pathway by promoting cell migration (Yang et al., 2016). Hence, future studies will be necessary to examine whether Caveolin-1 expression alters Notch signaling in EpiSCs.

Many bioactive molecules, including many growth factors, play a critical role in wound healing process (Diegelmann and Evans, 2004). Among these molecules, EGF is one of the well-known factors for wound healing process. EGF is a key promoter associated with keratinocyte proliferation and differentiation at the wound site to accelerate wound healing and skin appendages regeneration (Santoro and Gaudino, 2005; Shikiji et al., 2003). In addition, EGF may contribute to the development and regeneration of sweat glands, a challenge in deep burn recovery (Li et al., 2002; Sheng et al., 2009). Our results further support the importance of EGF in skin burn wound healing by showing that EGF treatment promotes EpiSCs cell proliferation. Interestingly, these effects were promoted by overexpression of Caveolin-1 in EpiSCs. Interestingly, previous studies have shown that overexpression of Caveolin-1 in MCF-7 breast cancer cells resulted in higher EGF-induced proliferative and motility rates (Agelaki et al., 2009). Up-regulation of Caveolin-1 attenuates EGF signaling in senescent cells (Park et al., 2000). Overexpression of Caveolin-1 significantly inhibits the proliferation, migration, and invasion potential of human colorectal cancer cells by reducing EGF-induced EGFR activation (Yang et al., 2018). These studies together suggested that the interaction of Caveolin-1 and EGF may have cell-specific outcomes. Hence, future studies will be important to examine the functional interaction of Caveolin-1 and EGF signaling in EpiSCs. Further, it should also be noted that other factor, such as fibroblast growth factor (FGF) may also induce rapid closure of burn wounds (Ishikawa et al., 2006; Moya et al., 2010). Actually, FGF stimulates keratinocyte division in vitro and increases the proliferation of fibroblast and capillary endothelial cells, as well as collagen synthesis, granulation tissue formation and epidermal regeneration in vivo (Barrientos et al., 2008; Ishikawa et al., 2006; Wang et al., 2008). Hence, future studies will be important to examine the effects of these factors on Caveolin-1 mediated signaling and their contribution in EpiSC-induced skin wound healing.

In summary, our results demonstrated that Caveolin-1 expression level in EpiSCs contributes to EpiSC proliferation potential, and manipulation of EpiSC proliferation potential may be an effective approach to promote skin wound healing. However, when we focus on skin wound heal, it is also important to consider the quality of the wound healing process by avoiding scar formation. Our recent study showed that FGF reduces scar by inhibiting the differentiation of EpiSCs to myofibroblasts. Hence, combinational approach by using multiple growth factors and manipulation of EpiSC proliferation potential, we may develop effective and better therapies to promote the quality of skin wound recovery.

Acknowledgements

This paper was supported by the National Natural Science Foundation of China (Grant nos. 81772136, 81671970, 81671935) and Foundation of Guangdong Province, China (Grant no. 2017ZC0466) and Foundation of Foshan City, China (Grant no. 2017AG100181).

Declarations of interests

The authors have declared that no competing interests exist.

References

Agelaki, S., Spiliotaki, M., Markomanolaki, H., Kallergi, G., Mavroudis, D., Georgoulias, V., Stournaras, C., 2009. Caveolin-1 regulates EGFR signaling in MCF-7 breast cancer cells and enhances gefitinib-induced tumor cell inhibition. Cancer Biol. Ther. 8, 1470–1477.

Baker, N., Zhang, G., You, Y., Tuan, R.S., 2012. Caveolin-1 regulates proliferation and osteogenic differentiation of human mesenchymal stem cells. J. Cell. Biochem. 113, 3773–3787.

Barrientos, S., Stojadinovic, O., Golinko, M.S., Brem, H., Tomic-Canic, M., 2008. Growth factors and cytokines in wound healing. Wound Repair Regen. 16, 585–601.

Blanpain, C., Fuchs, E., 2009. Epidermal homeostasis: a balancing act of stem cells in the skin. Nat. Rev. Mol. Cell Biol. 10, 207–217.

Borue, X., Lee, S., Grove, J., Herzog, E.L., Harris, R., Diflo, T., Glusac, E., Hyman, K., Theise, N.D., Krause, D.S., 2004. Bone marrow-derived cells contribute to epithelial engraftment during wound healing. Am. J. Pathol. 165, 1767–1772.

Boscher, C., Nabi, I.R., 2012. Caveolin-1: role in cell signalingCaveolins and Caveolae. Springer, 29–50.

Calum, H., Høiby, N., Moser, C., 2014. Burn mouse modelsPseudomonas Methods and Protocols. Springer, 793–802.

Case, N., Xie, Z., Sen, B., Styner, M., Zou, M., O'Conor, C., Horowitz, M., Rubin, J., 2010. Mechanical activation of beta-catenin regulates phenotype in adult murine marrow-derived mesenchymal stem cells. J. Orthop. Res. 28, 1531–1538.

Charruyer, A., Ghadially, R., 2011. What's new in dermatology: epidermal stem cells. G. Ital. Dermatol. Venereol.: Organo Uff. Soc. Ital. Dermatol. Sifilogr. 146, 57–67.

Chen, M., Przyborowski, M., Berthiaume, F., 2009. Stem cells for skin tissue engineering and wound healing. Crit. Rev.™ Biomed. Eng. 37.

Codenotti, S., Vezzoli, M., Poliani, P.L., Cominelli, M., Bono, F., Kabbout, H., Faggi, F., Chiarelli, N., Colombi, M., Zanella, I., Biasiotto, G., Montanelli, A., Caimi, L., Monti, E., Fanzani, A., 2016. Caveolin-1, Caveolin-2 and Cavin-1 are strong predictors of adipogenic differentiation in human tumors and cell lines of liposarcoma. Eur. J. Cell Biol. 95, 252–264.

Diegelmann, R.F., Evans, M.C., 2004. Wound healing: an overview of acute, fibrotic and delayed healing. Front. Biosci. 9, 283–289.

Du, J., Chen, X., Liang, X., Zhang, G., Xu, J., He, L., Zhan, Q., Feng, X.-Q., Chien, S., Yang, C., 2011. Integrin activation and internalization on soft ECM as a mechanism of induction of stem cell differentiation by ECM elasticity. Proc. Natl. Acad. Sci. USA, 201106467.

Eckert, R.L., Adhikary, G., Balasubramanian, S., Rorke, E.A., Vemuri, M.C., Boucher, S.E., Bickenbach, J.R., Kerr, C., 2013. Biochemistry of epidermal stem cells. Biochim. Biophys. Acta (BBA)-Gen. Subj. 1830, 2427–2434.

Fridolfsson, H.N., Roth, D.M., Insel, P.A., Patel, H.H., 2014. Regulation of intracellular signaling and function by caveolin. FASEB J. 28, 3823–3831.

Fu, Y., Moore, X.-L., Lee, M.K., Fernández-Rojo, M.A., Parat, M.-O., Parton, R.G., Meikle, P.J., Sviridov, D., Chin-Dusting, J.P., 2012. Caveolin-1 plays a critical role in the differentiation of monocytes into macrophages. Arterioscler. Thromb., Vasc. Biol. 32, e117–e125.

Fuchs, S., Hollins, A., Laue, M., Schaefer, U., Roemer, K., Gumbleton, M., Lehr, C.-M., 2003. Differentiation of human alveolar epithelial cells in primary culture: morphological characterization and synthesis of caveolin-1 and surfactant protein-C. Cell Tissue Res. 311, 31–45.

Fujita, Y., Maruyama, S., Kogo, H., Matsuo, S., Fujimoto, T., 2004. Caveolin-1 in mesangial cells suppresses MAP kinase activation and cell proliferation induced by bFGF and PDGF. Kidney Int. 66, 1794–1804.

Galbiati, F., Volonte', D., Liu, J., Capozza, F., Frank, P.G., Zhu, L., Pestell, R.G., Lisanti, M.P., 2001. Caveolin-1 expression negatively regulates cell cycle progression by inducing G0/G1 arrest via a p53/p21WAF1/Cip1-dependent mechanism. Mol. Biol. Cell 12, 2229–2244.

Gurel, A., Armutcu, F., Hosnuter, M., Unalacak, M., Kargi, E., Altinyazar, C., 2004. Caffeic acid phenethyl ester improves oxidative organ damage in rat model of thermal trauma. Physiol. Res. 53, 675–682.

Ishikawa, T., Terai, S., Urata, Y., Marumoto, Y., Aoyama, K., Sakaida, I., Murata, T., Nishina, H., Shinoda, K., Uchimura, S., 2006. Fibroblast growth factor 2 facilitates the differentiation of transplanted bone marrow cells into hepatocytes. Cell Tissue Res. 323, 221–231.

Jasmin, J.F., Yang, M., Iacovitti, L., Lisanti, M.P., 2009. Genetic ablation of caveolin-1 increases neural stem cell proliferation in the subventricular zone (SVZ) of the adult mouse brain. Cell Cycle 8, 3978–3983.

Kanji, S., Das, H., 2017. Advances of stem cell therapeutics in cutaneous wound healing and regeneration. Mediat. Inflamm., 2017.
Lee, M.Y., Ryu, J.M., Lee, S.H., Park, J.H., Han, H.J., 2010. Lipid rafts play an important role for maintenance of embryonic stem cell self-renewal. J. Lipid Res. 51, 2082–2089.
Li, J., Fu, X., Sun, X., Sun, T., Sheng, Z., 2002. The interaction between epidermal growth factor and matrix metalloproteinases induces the development of sweat glands in human fetal skin. J. Surg. Res. 106, 258–263.
Li, J., Hassan, G.S., Williams, T.M., Minetti, C., Pestell, R.G., Tanowitz, H.B., Frank, P.G., Sotgia, F., Lisanti, M.P., 2005. Loss of caveolin-1 causes the hyper-proliferation of intestinal crypt stem cells, with increased sensitivity to whole body γ-radiation. Cell Cycle 4, 1817–1825.
Li, Y., Lau, W.-M., So, K.-F., Tong, Y., Shen, J., 2011a. Caveolin-1 inhibits oligodendroglial differentiation of neural stem/progenitor cells through modulating β-catenin expression. Neurochem. Int. 59, 114–121.
Li, Y., Lau, W.-M., So, K.-F., Tong, Y., Shen, J., 2011b. Caveolin-1 promote astroglial differentiation of neural stem/progenitor cells through modulating Notch1/NICD and Hes1 expressions. Biochem. Biophys. Res. Commun. 407, 517–524.
Li, Y., Luo, J., Lau, W.M., Zheng, G., Fu, S., Wang, T.T., Zeng, H.P., So, K.F., Chung, S.K., Tong, Y., Liu, K., Shen, J., 2011c. Caveolin-1 plays a crucial role in inhibiting neuronal differentiation of neural stem/progenitor cells via VEGF signaling-dependent pathway. PLoS One 6, e22901.
Liu, Z., Xu, Y., Chen, L., Xie, J., Tang, J., Zhao, J., Shu, B., Qi, S., Chen, J., Liang, G., 2016. Dendritic epidermal T cells facilitate wound healing in diabetic mice. Am. J. Transl. Res. 8, 2375.
Moya, M.L., Garfinkel, M.R., Liu, X., Lucas, S., Opara, E.C., Greisler, H.P., Brey, E.M., 2010. Fibroblast growth factor-1 (FGF-1) loaded microbeads enhance local capillary neovascularization. J. Surg. Res. 160, 208–212.
Ng, Y.-S., Ramsauer, M., Loureiro, R.M.B., D'Amore, P.A., 2004. Identification of genes involved in VEGF-mediated vascular morphogenesis using embryonic stem cell-derived cystic embryoid bodies. Lab. Investig. 84, 1209–1218.
Odajima, N., Betsuyaku, T., Nasuhara, Y., Nishimura, M., 2007. Loss of caveolin-1 in bronchiolization in lung fibrosis. J. Histochem. Cytochem. 55, 899–909.
Park, J.H., Han, H.J., 2009. Caveolin-1 plays important role in EGF-induced migration and proliferation of mouse embryonic stem cells: involvement of PI3K/Akt and ERK. Am. J. Physiol.-Cell Physiol. 297, C935–C944.
Park, J.H., Ryu, J.M., Han, H.J., 2011. Involvement of caveolin-1 in fibronectin-induced mouse embryonic stem cell proliferation: role of FAK, RhoA, PI3K/Akt, and ERK 1/2 pathways. J. Cell. Physiol. 226, 267–275.
Park, J.S., Kim, H.Y., Kim, H.W., Chae, G.N., Oh, H.T., Park, J.Y., Shim, H., Seo, M., Shin, E.Y., Kim, E.G., Park, S.C., Kwak, S.J., 2005. Increased caveolin-1, a cause for the declined adipogenic potential of senescent human mesenchymal stem cells. Mech. Ageing Dev. 126, 551–559.
Park, W.Y., Park, J.S., Cho, K.A., Kim, D.I., Ko, Y.G., Seo, J.S., Park, S.C., 2000. Up-regulation of caveolin attenuates epidermal growth factor signaling in senescent cells. J. Biol. Chem. 275, 20847–20852.
Reiisi, S., Esmaeili, F., Shirazi, A., 2010. Isolation, culture and identification of epidermal stem cells from newborn mouse skin. Vitr. Cell. Dev. Biol.-Anim. 46, 54–59.
Robert-Moreno, A., Guiu, J., Ruiz-Herguido, C., Lopez, M.E., Ingles-Esteve, J., Riera, L., Tipping, A., Enver, T., Dzierzak, E., Gridley, T., Espinosa, L., Bigas, A., 2008. Impaired embryonic haematopoiesis yet normal arterial development in the absence of the Notch ligand Jagged1. EMBO J. 27, 1886–1895.
Rubin, J., Schwartz, Z., Boyan, B.D., Fan, X., Case, N., Sen, B., Drab, M., Smith, D., Aleman, M., Wong, K.L., 2007. Caveolin-1 knockout mice have increased bone size and stiffness. J. Bone Miner. Res. 22, 1408–1418.
Samarasinghe, R.A., Di Maio, R., Volonte, D., Galbiati, F., Lewis, M., Romero, G., DeFranco, D.B., 2011. Nongenomic glucocorticoid receptor action regulates gap junction intercellular communication and neural progenitor cell proliferation. Proc. Natl. Acad. Sci. USA 108, 16657–16662.
Santoro, M., Gaudino, G., 2005. Cellular and molecular facets of keratinocyte reepithelization during wound healing. Exp. Cell Res. 304, 274–286.
Sheng, Z., Fu, X., Cai, S., Lei, Y., Sun, T., Bai, X., Chen, M., 2009. Regeneration of functional sweat gland-like structures by transplanted differentiated bone marrow mesenchymal stem cells. Wound Repair Regen. 17, 427–435.
Shi, Y., Shu, B., Yang, R., Xu, Y., Xing, B., Liu, J., Chen, L., Qi, S., Liu, X., Wang, P., 2015. Wnt and Notch signaling pathway involved in wound healing by targeting c-Myc and Hes1 separately. Stem Cell Res. Ther. 6, 120.
Shikiji, T., Minami, M., Inoue, T., Hirose, K., Oura, H., Arase, S., 2003. Keratinocytes can differentiate into eccrine sweat ducts in vitro: involvement of epidermal growth factor and fetal bovine serum. J. Dermatol. Sci. 33, 141–150.
Sotgia, F., Williams, T.M., Cohen, A.W., Minetti, C., Pestell, R.G., Lisanti, M.P., 2005. Caveolin-1-deficient mice have an increased mammary stem cell population with upregulation of Wnt/?-catenin signaling. Cell Cycle 4, 1808–1816.
Wang, P., Shu, B., Xu, Y., Zhu, J., Liu, J., Zhou, Z., Chen, L., Zhao, J., Liu, X., Qi, S., 2017. Basic fibroblast growth factor reduces scar by inhibiting the differentiation of epidermal stem cells to myofibroblasts via the Notch1/Jagged1 pathway. Stem Cell Res. Ther. 8, 114.
Wang, S., Kan, Q., Sun, Y., Han, R., Zhang, G., Peng, T., Jia, Y., 2013. Caveolin-1 regulates neural differentiation of rat bone mesenchymal stem cells into neurons by modulating Notch signaling. Int. J. Dev. Neurosci. 31, 30–35.
Wang, W., Lin, S., Xiao, Y., Huang, Y., Tan, Y., Cai, L., Li, X., 2008. Acceleration of diabetic wound healing with chitosan-crosslinked collagen sponge containing recombinant human acidic fibroblast growth factor in healing-impaired STZ diabetic rats. Life Sci. 82, 190–204.
Williams, T.M., Lisanti, M.P., 2004. The caveolin proteins. Genome Biol. 5, 214.
Yang, J., Zhu, T., Zhao, R., Gao, D., Cui, Y., Wang, K., Guo, Y., 2018. Caveolin-1 inhibits proliferation, migration, and invasion of human colorectal cancer cells by suppressing phosphorylation of epidermal growth factor receptor. Med. Sci. Monit. 24, 332–341.
Yang, R.-H., Qi, S.-H., Shu, B., Ruan, S.-B., Lin, Z.-P., Lin, Y., Shen, R., Zhang, F.-G., Chen, X.-D., Xie, J.-L., 2016. Epidermal stem cells (ESCs) accelerate diabetic wound healing via the Notch signaling pathway. Biosci. Rep., (BSR20160034).
Zhu, H., Wei, X., Bian, K., Murad, F., 2008. Effects of nitric oxide on skin burn wound healing. J. Burn Care Res. 29, 804–814.